Study of (Tetraphenylporphinato)manganese(III)-Catalyzed Epoxidation and Demethylation Using *p*-Cyano-*N*,*N*-dimethylaniline *N*-Oxide as Oxygen Donor in a Homogeneous System. Kinetics, Radiochemical Ligation Studies, and Reaction Mechanism for a Model of Cytochrome P-450

Michael F. Powell, Emil F. Pai, and Thomas C. Bruice*

Contribution from the Department of Chemistry, University of California at Santa Barbara, Santa Barbara, California 93106. *Received September 23, 1983*

Abstract: Oxygen transfer from *p*-cyanodimethylaniline (*p*-CNDMANO) to cyclohexene as well as "intramolecular" oxygen transfer accompanied by demethylation to yield *p*-cyanomonomethylaniline (*p*-CNMMA) are strongly catalyzed by ligated (tetraphenylporphinato)Mn^{III} (i.e., $XMn^{III}TPP$). These reactions have been studied in dry, oxygen-free benzonitrile. Radiochemical studies show that H_2O (or TOH) is not bound to $XMn^{III}TPP$ in aprotic solvents so that the Mn^{III} moiety is pentacoordinate. Oxygen transfer occurs through the reversible formation of the hexacoordinated species *p*-CNDMANO·$Mn^{III}(X)TPP$. This species decomposes to *p*-cyanodimethylaniline (*p*-CNDMA) + $O{=}Mn^{V}(X)TPP$. Reaction of cyclohexene with $O{=}Mn^{V}(X)TPP$ yields cyclohexene epoxide and $XMn^{III}TPP$ whereas *p*-CNMMA is formed directly from the *p*-CNDMANO·$Mn^{III}(X)TPP$ complex. The rates of product formation are shown to be dependent upon the nature of the ligand (X^- = F^-, Cl^-, Br^-, I^-, OCN^-). In the absence of the axial ligand X^-, the rates of reaction are extremely slow. Thus, the Mn^{III} C_2-cap-porphyrin ($XMn^{III}CAPTPP$), which can only form an $O{=}Mn^{V}$ porphyrin species wherein the Mn moiety is not complexed to X^- as a sixth ligand, shows almost no tendency to act as a catalyst for oxygen transfer. The necessary presence of the axial ligand X^- and the dependence of rate upon X^- requires the structure of the oxygen transfer species to be quivalent to $O{=}Mn^{V}(X)TPP$. A kinetic analysis is presented (Scheme III) which has allowed the determination of the influence of the ligands X^- upon the various rate constants (Table IV) involved in the overall oxidations. By employing *p*-CNDMANO as oxygen donor, multiple catalytic turnovers without loss of porphyrin have been realized.

Introduction

The ability of cytochrome P-450 to activate dioxygen with resultant oxygen transfer to otherwise relatively unreactive organic substrates has attracted much attention.[1] Although the detailed mechanism of the oxygen transfer is not yet understood fully, the generation of higher valent oxidizing species in model systems by the use of a wide variety of "oxene" transfer agents, including iodosobenzene, peroxy acids, hydrogen peroxide, and activated *N*-oxides,[2] indicates that oxo-Fe intermediates may be involved in the mechanism of cytochrome P-450. That Mn provides a reasonable substitute for Fe in model studies of cytochrome P-450 was recently demonstrated when Gelb et al.[3] prepared Mn-substituted cytochrome $P\text{-}450_{cam}$ ($P\text{-}450_{cam}$ = *P. putida* ATCC 29607) which acts as a catalyst for the epoxidation of enzyme-bound alkene substrate in the presence of iodosobenzene as oxygen donor. Furthermore, reaction was observed to proceed via a spectrally detectable intermediate which closely resembled the manganese(V)–oxo complexes found to be present in earlier model studies (loc. cit.). The necessity of manganese for oxygen evolution in the photosynthetic process[4] has also encouraged studies of manganese porphyrins. Although the exact role of Mn in photosynthesis is still unknown, it has often been suggested that higher valent oxo–manganese species may be involved.

Evidence for the existence of high-valence Mn–porphyrin complexes was provided when Willner et al.[5] isolated oxomanganesetetraphenylporphyrin ($O{=}Mn^{IV}(X)TPP$) from the reaction of $Mn^{III}TPP$ and iodosobenzene. Subsequently, it was shown that treatment of $ClMn^{III}TPP$ with iodosobenzene gave pentavalent oxomanganesetetraphenylporphyrin chloride ($O{=}Mn^{V}(Cl)TPP$), a species which proved to be a powerful oxidant.[6] Other Mn–porphyrin-catalyzed oxidations include: (i) dioxygenation of alkyl-substituted indoles by $ClMn^{III}TPP$[7] and phthalocyanins [$Mn^{III}(PC)$][8] using O_2 as the oxygen source; (ii) reaction of $ClMn^{III}TPP$ with $NaBH_4$ and O_2 to convert cyclohexene to cyclohexanol and cyclohexen-3-ol;[9] (iii) oxidation of γ,δ-unsaturated ketones by O_2 and Mn^{III} (salen) [salen = bis(salicylidene)ethylenediaminato] to give enediones;[10] (iv) oxidation of various alkenes to ketones by $ClMn^{III}TPP$, NBu_4^+, and BH_4^- in the presence of O_2;[11] (v) formation of triphenylphosphine oxide (PPh_3O) from PPh_3 and $O{=}Mn^{IV}TPP$;[5] (vi) alkane activation and functionalization by use of $XMn^{III}TPP$ (X^- = Cl^-, Br^-, I^-, N_3^-) with iodosobenzene;[12-14] (vii) study of metalloporphyrin-

(1) For recent reviews see: (a) Coon, M. J.; White, R. E. "Metal Ion Activation of Dioxygen"; Spiro, T. G., Ed.; Wiley: New York, 1980. (b) Gunsalus, J. C.; Sligar, S. G. *Adv. Enzymol. Relat. Areas Mol. Biol.* **1978**, *47*, 1–44. (c) Groves, J. T. *Adv. Inorg. Biochem.* **1979**, *1*, 119–145.

(2) (a) Nee, M. W.; Bruice, T. C. *J. Am. Chem. Soc.* **1982**, *104*, 6123–6125. (b) Groves, J. T.; Nemo, T. E.; Myers, R. S. *Ibid.* **1979**, *101*, 1032–1033. (c) Chang, C. K.; Kuo, M.-S. *Ibid.* **1979**, *101*, 3413–3415. (d) Mansuy, D.; Bartoli, J.-F.; Chottard, J.-C.; Lange, M. *Angew. Chem., Int. Ed. Engl.* **1980**, *19*, 909–910. (e) Mansuy, D.; Dansette, P. M.; Pecquet, F.; Chottard, J.-C. *Biochem. Biophys. Res. Commun.* **1980**, *96*, 433–439. (f) Gold, A.; Ivey, W.; Brown, M. *J. Chem. Soc., Chem. Commun.* **1981**, 293–295. (g) Chang, C. K.; Ebina, F. *Ibid.* **1981**, 778–779. (h) Groves, J. T.; Haushalter, R. C.; Nakamura, M.; Nemo, T. E.; Evans, B. J. *J. Am. Chem. Soc.* **1981**, *103*, 2884–2886. (i) Lindsay Smith, J. R.; Sleath, P. R. *J. Chem. Soc., Perkin Trans. 2* **1982**, 1009–1015.

(3) Gelb, M. H.; Toscano, W. A., Jr.; Sligar, S. G. *Proc. Natl. Acad. Sci. U.S.A.* **1982**, *79*, 5758–62.

(4) For example, see: Livorness, J.; Smith, T. D. *Struct. Bonding (Berlin)* **1982**, *48*, 1–44.

(5) Willner, I.; Otvos, J. W.; Calvin, M. *J. Chem. Soc., Chem. Commun.* **1980**, 964–5.

(6) Groves, J. T.; Kruper, W. J., Jr.; Haushalter, R. C. *J. Am. Chem. Soc.* **1980**, *102*, 6375–7.

(7) Dufour, M. N.; Crumbliss, A. L.; Johnston, G.; Gaudemer, A. *J. Mol. Catal.* **1980**, *7*, 277–287.

(8) Uchida, K. Soma, M.; Naito, S.; Onishi, T.; Tamaru, K. *Chem. Lett.* **1978**, 471–474.

(9) Tabushi, I.; Koga, N. *J. Am. Chem. Soc.* **1979**, *101*, 6456–6458.

(10) Costantini, M.; Dromard, A.; Jouffret, M.; Brossard, B.; Varagnat, J. *J. Mol. Catal.* **1980**, *7*, 89–97.

(11) Perree-Fauvet, M.; Gaudemer, A. *J. Chem. Soc., Chem. Commun.* **1981**, 874.

(12) Hill, C. L.; Schardt, B. C. *J. Am. Chem. Soc.* **1980**, *102*, 6374–6375.

(13) Smegal, J. A.; Schardt, B. C.; Hill, C. L. *J. Am. Chem. Soc.* **1983**, *105*, 3510–15.

(14) Smegal, J. A.; Hill, C. L. *J. Am. Chem. Soc.* **1983**, *105*, 3515–21.

0002-7863/84/1506-3277$01.50/0

catalyzed alkane hydroxylation with alkyl hydroperoxides and iodosobenzene;[15] (viii) activation of sodium hypochlorite by $AcOMn^{III}TPP$ (AcO^- = acetate);[16] (ix) reaction of $XMn^{III}TPP$ with ArCOCl to give a Mn^{III} acylperoxy complex which is proposed to yield $O{=}Mn^{V}(HO)TPP$ in the presence of HO^-;[17] and (x) alkane activation and hydroxylation by a $ClMn^{III}TPP$–ascorbate biphasic system.[18] These studies have shown that the specificity for substrates is dependent upon the nature of the oxygen source. For example, reaction of iodosobenzene and $ClMn^{III}TPP$ is thought to more closely model cytochrome P-450 than the reaction of alkyl hydroperoxide with $ClMn^{III}TPP$ which apparently follows a "Fenton-type" mechanism.[15]

Numerous spectral investigations firmly establish that thiol anion is an axial ligand of iron protoporphyrin in cytochrome P-450's and there has been much speculation about its role.[19-23] Systematic ligand variation in porphyrins has been shown to affect the reduction–oxidation potentials of both the metal[24] and macrocycle,[25] the binding constants of substrates and inhibitors,[26] activation of effector molecules such as oxygen,[27] and, of course, the porphyrin spectral features.[28] Much of the pioneering work in the determination of the physical properties of axially substituted Mn porphyrins was carried out by Boucher.[28,29] It is to be expected that the axial ligand of metalloporphyrins should have a noticeable effect on oxene transfer in model systems since the oxy intermediate must involve some metal-centered oxidation.

In this paper we report the effect of the ligand on the rates of epoxidation and N-demethylation for a cytochrome P-450 model system. In this initial investigation we have chosen to use Mn^{III} porphyrins rather than Fe^{III} porphyrins. This choice is based on the lack of affinity of Mn^{III} porphyrins for a sixth axial ligand. This feature greatly simplifies detailed kinetic studies because it ensures that X_2Mn^{III} porphyrin species do not accumulate en route to the formation of $O{=}Mn^{V}(X)$ porphyrin. The porphyrin systems employed are X^- ligated Mn^{III} tetraphenylporphyrin ($XMn^{III}TPP$) and the Mn^{III} C_2-capporphyrin of Baldwin[30] ($XMn^{III}CAPTPP$) which can only form an $O{=}Mn^{V}$ porphyrin

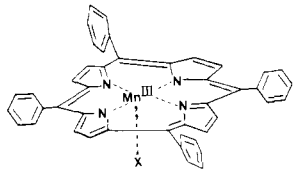

$XMn^{III}TPP$

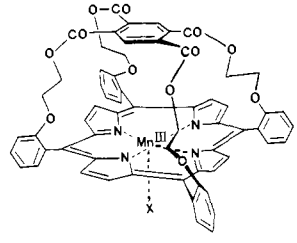

$XMn^{III}CAPTPP$

species uncomplexed to X^-. We chose the *N*-oxide of *p*-cyano-*N*,*N*-dimethylaniline[2a] (*p*-CNDMANO) as the oxygen donor to the Mn^{III} porphyrins since (i) *N*-oxides have some important advantages over iodoso aromatics as oxygen donors, particularly their higher solubility in organic solvents, their monomeric nature, and their inability to oxidatively destroy the porphyrin ring (as iodosobenzene does in absence of excess substrate[2b]), and (ii) epoxidation and hydroxylation yields using p-CNDMANO are virtually identical with those of iodosobenzene and significantly higher than with *N*,*N*-dimethylaniline *N*-oxide (DMANO), the first *N*-oxide used to show oxygen donation ability to P-450 model systems.[2b] This initial report demonstrates that a systematic study of reaction rates of oxygen transfer in homogeneous porphyrin reaction systems can be achieved, providing the primary oxygen donor (*p*-CNDMANO), porphyrins, and solvent (PhCN) are chosen carefully.

Experimental Section

Physical Measurements. UV–visible spectra were recorded on a Cary 118C spectrophotometer equipped with a constant-temperature cell holder maintained at 30 °C. In most instances, spectra were in CH_2Cl_2, $CHCl_3$, or benzonitrile. Soret bands observed for $XMn^{III}TPP$ in the halo solvents were usually identical (to within 0.5 nm) and were often 1–2 nm lower than those obtained in benzonitrile. Fast atom bombardment mass spectra (FAB MS) were obtained from the laboratory of Dr. Rinehart at the University of Illinois. Gas chromatographic analyses were performed using a Varian Model 3700 gas chromatograph equipped with a FID detector and a Varian Model CDS101 integrator. Helium was used as the carrier gas. Liquid scintillation counting was done in 20-mL plastic vials using a Beckman liquid scintillation counter.

Materials. Benzonitrile (PhCN) and carbon disulfide (CS_2) were of spectrophotometric grade (Aldrich) and were dried over molecular sieves and deoxygenated before use. Reagent grade carbon tetrachloride (CCl_4) was dried over anhydrous $MgSO_4$ and distilled under N_2. Cyclohexene epoxide (CH-epox), cyclohexen-3-ol (CH-enol), and cyclohexen-3-one (CH-enone) were of reagent grade (Aldrich) and were used without further purification. Cyclohexene (CH-ene) was washed with 1 M NaOH, dried with anhydrous $MgSO_4$, refluxed over freshly powdered NaOH (2 h), and distilled (81 °C, uncorrected) before use. Gas chromatography showed only one very minor contaminant, possibly cyclohexanone, which did not interfere with the analysis of reaction samples. *p*-Cyanodimethylaniline *N*-oxide[31] (*p*-CNDMANO) was available in our laboratory[2a] and was recrystallized under a dry N_2 atmosphere from ethyl acetate–hexane. *p*-Cyanodimethylaniline (*p*-CNDMA) (Aldrich) was recrystallized from ethanol–diethyl ether. The analogous monomethylaniline (*p*-CNMMA) was from a previous study.[2a] Tetraphenylporphyrin (TPP) and 5,10,15,20-tetrakis(*p*-methoxyphenyl)porphyrin (MeOTPP) were obtained commercially from Aldrich. The C_2-cap-porphyrin (CAPTPP) used herein was prepared by the method of Baldwin.[30]

Synthesis of Mn Porphyrins. Tetraphenylporphinatomanganese chloride ($ClMn^{III}TPP$) and the acetate analogue ($OAcMn^{III}TPP$) were prepared using a modified procedure of Adler;[32] ligand exchange was accomplished in a manner similar to that described by Ogoshi et al.[33] Into 100 mL of purified dimethylformamide (DMF) were added ~0.5 g of porphyrin and a 2- to 20-fold molar excess of $Mn(OAc)_2$. The mixture was refluxed (or heated in a bomb to reflux temperature) for approximately 5 h. The DMF was removed by high-vacuum rotary evaporation and the residue extracted with a mixture of NaX–H_2O/$CHCl_3$ (X^- = F^-, Cl^-, Br^-, I^-, N_3^-, OAc^-, OCN^-, CN^-). After shaking for several minutes, the aqueous phase was separated and the $CHCl_3$ removed by rotary evaporation. An attempt was made to purify the product by column chromatography using $CHCl_3$ (containing 0.75% EtOH)–neutral alumina (3 cm × 30 cm); however, the dark green eluate was always $ClMn^{III}TPP$ regardless of the original porphyrin prepared in the NaX–H_2O/$CHCl_3$ wash. [This demonstrates that the usual[28] chromatographic purification for Mn porphyrins is unsatisfactory for the preparation of $XMn^{III}TPP$ (where $X^- \neq Cl$)]. Subsequent ligand exchange in NaX–H_2O/$CHCl_3$ afforded pure $XMn^{III}TPP$. (Contrary to earlier accounts,[28] we note that $CNMn^{III}TPP$ could also be prepared by this method; a recent report[34] on the X-ray structure of $CNMn^{III}TPP$

(15) Mansuy, D.; Bartoli, J.-F.; Momenteau, M. *Tetrahedron Lett.* **1982**, *23*, 2781–4.
(16) Guilmet, E.; Meunier, B. *Tetrahedron Lett.* **1982**, *23*, 2449–52.
(17) Groves, J. T.; Watanabe, Y.; McMurry, T. J. *J. Am. Chem. Soc.* **1983**, *105*, 4489–90.
(18) Mansuy, D.; Fontecave, M.f Bartoli, J.-F. *J. Chem. Soc., Chem. Commun.* **1983**, 253–4.
(19) Hanson, L. K.; Eaton, W. A.; Sligar, S. G.; Gunsalus, I. C.; Gouterman, M.; Connell, C. R. *J. Am. Chem. Soc.* **1976**, *98*, 2672–2674.
(20) Hanson, L. K. *Int. J. Quantum Chem., Quantum Biol. Symp.* **1979**, *6*.
(21) Yonetani, T.; Yamamoto, H.; Erman, J. E.; Leigh, J. S., Jr.; Reed, G. H. *J. Biol. Chem.* **1972**, *247*, 2447–2455.
(22) Ullrich, V.; Castle, L.; Hawand, M. In "Oxygenases and Oxygen Metabolism"; Nozaki, M., et al., Eds.; Academic Press: New York, 1982.
(23) Stern, J. O.; Peisach, J. *FEBS Lett.* **1976**, *62*, 364–8.
(24) Felton, R. H. In "The Porphyrins", Dolphin, D., Ed.; Academic Press: New York, 1978; Vol. 5, p 53.
(25) Davis, M. S.; Forman, A.; Fajer, J. *Proc. Natl. Acad. Sci. U.S.A.* **1979**, *76*, 4170–4174.
(26) Antonini, E.; Brunori, M. "Hemoglobin and Myoglobin in Their Reactions with Ligands"; Elsevier/North Holland: New York, 1971.
(27) Hayaishi, O., Ed. "Molecular Mechanisms of Oxygen Activation"; Academic Press: New York, 1974.
(28) Boucher, L. J. *Coord. Chem. Rev.* **1972**, *7*, 289–329.
(29) Boucher, L. J. *Ann. N.Y. Acad. Sci.* **1973**, *206*, 409–19.
(30) Almog, J.; Baldwin, J. E.; Crossley, M. J.; Debernardis, J. F.; Dyer, R. L.; Huff, J. R.; Peters, M. K. *Tetrahedron* **1981**, *37*, 3589–3601.
(31) Craig, J. C.; Purushothaman, K. K. *J. Org. Chem.* **1970**, *35*, 1721–1722.
(32) Adler, A. D.; Longo, F. R.; Kampas, F.; Kim, J. *J. Inorg. Nucl. Chem.* **1970**, *32*, 2443–2445.
(33) Ogoshi, H.; Watanabe, E.; Yoshida, Z.; Kincaid, J. K.; Nakamoto, K. *J. Am. Chem. Soc.* **1973**, *95*, 2845–2849.
(34) Scheidt, W. R.; Lee, Y. J.; Luangdilok, W.; Haller, K. J.; Anzai, K.; Hatano, K. *Inorg. Chem.* **1983**, *22*, 1516–1522.

shows this also.) $ClMn^{III}CAPTPP$ was prepared by heating ~50 mg of CAPTPP in 100 mL of dry THF with a 50-fold molar excess of $MnCl_2$ to 150 °C (sealed bomb) for 24 h. Although some CAPTPP decomposition occurred (~10%), $ClMn^{III}CAPTPP$ was obtained in good yield (~70%) after pufication on a column of neutral alumina using $CHCl_3$ as eluent. That Mn was incorporated into the C_2-capped porphyrin was demonstrated by a FAB MS peak at 1089.21 ($MnCAPTTP^+$). Ligand exchange in $XMn^{III}CAPTPP$ was carried out in the same manner as for $XMn^{III}TPP$ and $XMn^{III}MeOTPP$; usually 5 min of vigorous shaking in an $NaX-H_2O/CHCl_3$ biphasic solvent system caused ~100% ligand exchange. Complete exchange, however, could not be carried out in a single extraction when a nucleophile with weak ligand-binding properties (such as I^-) was being substituted for a strongly bound ligand (such as OCN^-). The rate of ligand exchange appeared to be similar (to within an order of magnitude) for $XMn^{III}TPP$ and $XMn^{III}CAPTPP$ in the $NaX-H_2O/CHCl_3$ biphasic system.

Radiometric Water Assay. A typical experiment proceeded as follows: a 2.5×10^{-3} M solution of $XMn^{III}TPP$ ($X^- = Cl^-, Br^-, I^-, N_3^-, OAc^-$) in CCl_4 (2 mL) was added to a 1 M NaX solution ($X^- = Cl^-, Br^-, I^-, N_3^-, OAc^-$) (0.5 mL) in tritiated water (1.8×10^{-5} Ci), and the mixture was mechanically shaken for 1 h at room temperature. (Carbon tetrachloride was the solvent of choice because of (i) its ease of dissolution of $XMn^{III}TPP$, (ii) a density greater than 1 which allows simple extraction and separation steps, and (iii) the low solubility of H_2O (or TOH) in this solvent.) Variation of the shaking time did not affect the outcome of the experiment. After standing for 1 h, the CCl_4 layer was transferred to a snap-top plastic vial and allowed to stand for an additional hour before 0.80 mL of CCl_4 solution was removed by hypodermic syringe through the vial wall—a precaution against "free" TOH contamination. This volume was back-extracted with exactly 4 mL of H_2O by vigorous shaking for 1.5 h. The CCl_4 was then removed and the aqueous phase was washed 3× with CH_2Cl_2 to remove traces of XMnTPP; these intensely colored complexes act as strong quenchers during scintillation counting. The H_2O was then bubbled gently with a stream of N_2 to remove traces of CH_2Cl_2 which is also a quencher, albeit a milder one. An aliquot of this solution (2 mL) was then added to Bray's solution[35] (15 mL) and counted using a Beckman scintillation counter. Most of the experiments were carried out in series using four solutions containing 2.5×10^{-3} M solution of $XMn^{III}TPP$ and four without added $XMn^{III}TPP$. Sample radioactivity in each of the four samples varied by approximately 10–15%; the standard deviations reported herein were calculated using $\sigma = [(\sum_{i=1}^{n}(x_i - \bar{x})^2)^{1/2}/(n-1)]$ where $n = 4$. The radioactivity observed in experiments done without $XMn^{III}TPP$ present is attributed to traces of labeled H_2O dissolved in CCl_4 (water solubility ~0.1 wt % at 24 °C[36]). The UV spectra of the CCl_4 layer containing XMnTPP was run prior to (and after) shaking with saline tritiated water to ensure that the porphyrin did not decompose or undergo unwanted "fifth-ligand" exchange. In all experiments the initial and final spectra were identical. The low solubilities of $FMn^{III}TPP$ and NaF in CCl_4 and H_2O, respectively, prevented similar experiments being done with this porphyrin.

Ligand Exchange Measurements. A solution ~10^{-6} M in $FMn^{III}TPP$ was allowed to react with an approximately 10-fold excess of $ClMn^{III}MeOTPP$ in dry PhCN. The Soret band identified with $FMn^{III}TPP$ (λ 459 nm) was observed to move to 462 nm, close to that for $FMn^{III}MeOTPP$ (λ 462.5 nm). A similar experiment done with $FMn^{III}TPP$ and an approximately fourfold excess of $ClMn^{III}CAPTPP$ resulted in a Soret band shift from 459 to 462 nm, close to the λ_{max} (Soret) for $FMn^{III}CAPTPP$ (λ 463 nm). Reaction of $FMn^{III}TPP$ with an excess of $N_3Mn^{III}CAPTPP$ showed a Soret band shift from 459 to 462.5 nm. Whereas the exchange reaction with $ClMn^{III}TPP$ took place before the spectrum could be scanned (5 nm/s, 700–350 nm), the reaction with $N_3Mn^{III}CAPTPP$ required several minutes to reach completion, presumably owing to the higher ligand binding strength of the N_3 ligand.

Sonication of a H_2O-saturated CH_2Cl_2 solution of ~10^{-6} M $FMn^{III}TPP$ and solid NaCl resulted in a decrease in optical density at λ 457 nm ($FMn^{III}TPP$) and an increase at λ 476 nm ($ClMn^{III}TPP$) within 1 h. Analogous experiments with $ClMn^{III}TPP$ and solid NaF in wet CH_2Cl_2 gave no spectral change when sonicated for 24 h.

Kinetics. All manipulations were carried out under a dry N_2 atmosphere with solvents which were deoxygenated before use. To a known amount of *p*-CNDMANO in PhCN was added a solution of $XMn^{III}TPP$ and cyclohexene (CH-ene) in PhCN such that the final volume of 10 mL had the following concentrations: $[p\text{-CNDMANO}]_0 = 2 \times 10^{-2}$ M, $[CH\text{-ene}]_0 = 2$ M, and $[XMn^{III}TPP]_0 = 2 \times 10^{-3}$ M. The kinetic run was initiated ($t = 0$) upon mixing the temperature-equilibrated (23.5 °C) *p*-CNDMANO and $XMn^{III}TPP$ solutions. At known time intervals, aliquots of 250 μL were removed from the reaction solution and quenched by the rapid addition of exactly 250 μL of CS_2. (Control experiments demonstrated that CS_2 reacts quickly with *p*-CNDMANO under the conditions used herein.) Quenched samples were sealed in airtight septum top vials and stored at −22 °C under N_2 until GC analysis. The epoxide of cyclohexene (CH-epox), cyclohexen-3-ol (CH-enol), PhCN, and CS_2 were separated on a 2-m Varian Chromosorb 80/100 W-HP, 5% OV 17 column using a programmed temperature gradient (100 °C for 8 min, 28 °C/min up to 240 °C, 240 °C for 6 min). The methylanilines were analyzed on a 2-m Varian 10% Carbowax 20–5% KOH on Chromosorb W 17/W 80/100 column at 225 °C. Both columns were previously calibrated with PhCN solutions containing known concentrations of the reaction products. Both peak height and peak area were used to measure the concentrations of the various species; averaging of the two methods usually gave the most consistent and reliable results.

Calculations were performed on a Hewlett-Packard 9825A calculator equipped with a Hewlett-Packard Model 9864A digitizer and Model 9867A plotter. Reaction scheme simulations were carried out using a program[37] which, when fed with the appropriate rate constants and initial concentrations, calculated the change in concentrations of all the reaction species for a short time increment, dt, using the reaction scheme differential equations. These concentration changes were then subtracted from the original concentrations at the time t_0 giving new concentrations at time $t_0 + dt$. The calculation was then repeated many times until newly calculated values were no longer significantly different from previous values, i.e., until equilibrium was reached. The calculated concentrations were then plotted vs. time on an overlay of the experimental data, and a visual best fit was done.

Table I. Visible Absorption Soret Band Wavelengths (nm) for XMnTPP, $XMn^{III}MeOTPP$, and $XMn^{III}CAPTPP$ in CH_2Cl_2 at 30 °C

X	$XMn^{III}TPP$	$XMn^{III}MeOTPP$	$XMn^{III}CAPTPP$
F^-	456	460	462
Cl^-	476	480	483
Br^-	484	485	489
I^-	496		501
OCN^-	474		478
N_3^-	484		490
BF_4^-	458		462
OAc^-	468		
CN^-	496		

Results

Electronic Spectra. In contrast to the Fe^{III} porphyrins, the UV–visible spectra of the Mn^{III} porphyrins exhibit a strong ligand dependence on both the intense B (Soret) band wavelength[28] and extinction coefficient. We have found that measurement of the Soret band wavelength constitutes an acceptable method for the identification of the ligated Mn^{III} porphyrins in solution and have tabulated these for the porphyrins studied herein. Inspection of Table I shows that the capped porphyrins, $XMn^{III}CAPTPP$, do not display any unusual spectroscopic behavior; the λ_{max} values appear to be shifted to lower energy by 5 ± 1 nm when compared with $XMn^{III}TPP$.

The ability of H_2O to bind as a sixth axial ligand to $XMn^{III}TPP$ (eq 1) was investigated by shaking a CCl_4 solution of $XMn^{III}TPP$

$$XMn^{III}TPP + H_2O \overset{K_{H_2O}}{\rightleftharpoons} XMn^{III}(H_2O)TPP \qquad (1)$$

with an aqueous solution containing TOH and 1 M NaX and determining if the radioactivity in the CCl_4 is related to the $[XMn^{III}TPP]$ in this phase (see Experimental Section). $XMn^{III}TPP$ lacks normal[38] acid sites which may exchange with TOH under the neutral pH conditions employed so that an increase in radioactivity accompanying an increase in $[XMn^{III}TPP]$ in the organic phase must be attributed to the presence of $XMn^{III}(TOH)TPP$. Radioactivity found in CCl_4 without added $XMn^{III}TPP$ (as assayed for by counting a known volume of the second H_2O wash in order to eliminate quenching by CCl_4) is due

(35) Evans, E. A. "Tritium and its Compounds", 2nd ed.; Wiley: London, 1974.

(36) Steven, H.; Steven, T., Eds. "Solubilities of Inorganic and Organic Compounds"; Pergamon Press: Oxford, 1963; Vol. 1.

(37) This type of program is shown in: Powell, M. F. Ph.D. Thesis, University of Toronto, 1981.

(38) Eigen, M. *Angew. Chem., Int. Ed. Engl.* **1964**, *3*, 1–19.

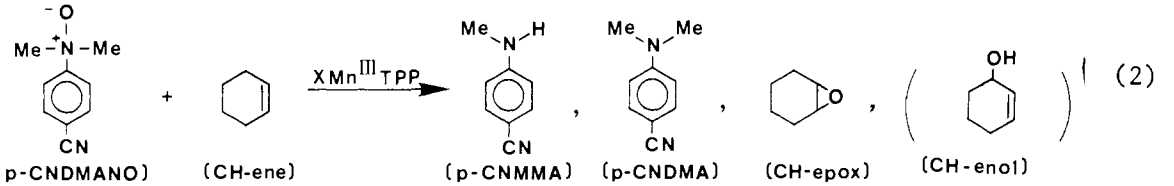

Table II. Summary of Calculated and Observed Counts per Minute (cpm) for $XMn^{III}TPP$ and $XMn^{III}(H_2O)TPP$ in CCl_4 Solution

X	calcd for $XMn^{III}TPP$ (control expt)	calcd for 2.5×10^{-3} M $XMn^{III}(H_2O)TPP$	obsd
Cl^-	870 ± 40	1620	770 ± 83
Br^-	760 ± 36	1415	773 ± 105
I^-	704 ± 89	1310	702 ± 49
N_3^-	867 ± 131	1615	881 ± 159
OAc^-	851 ± 48	1585	892 ± 128
F^-	too insoluble		

to the solubility of H_2O (and TOH) in CCl_4; indeed, the partitioning of H_2O into CCl_4 from salt solutions can be estimated by this method. The following calculation assumes the aqueous "tritium pool" is significantly larger than the amount of TOH in CCl_4 or in $XMn^{III}(TOH)TPP$. Control experiments showed that 0.5 mL of the TOH used herein had 2.08×10^7 cpm, whereas 0.4 mL of the CCl_4 fraction gave approximately 870 cpm. Thus, the amount of H_2O in 0.4 mL of CCl_4 is 870 cpm/2.08×10^7 cpm $\times$ 0.5 mL = 2.09×10^{-5} mL or 2.9×10^{-3} M. This value agrees fairly well with the literature value of $\sim 7 \times 10^{-3}$ M for the solubility of H_2O in CCl_4 when one considers the neglect of salt effects or isotopic fractionation on the solubility and partitioning of H_2O vs. TOH. Thus, if the counts are 870 cpm for a control experiment in which the CCl_4 solution contained 2.9×10^{-3} M H_2O but no added $XMn^{III}TPP$, then solutions containing 2.5×10^{-3} M $XMn^{III}TPP$ should display $\{(2.5 \times 10^{-3}$ M + 2.9×10^{-3} M)/2.9×10^{-3} M$\} \times 870$ cpm = 1620 cpm if $XMn^{III}TPP$ is converted to $XMn^{III}(H_2O)TPP$ and $\sim$870 cpm if no ligated H_2O is present. Similarly, sample counts should vary between 870 and 1620 cpm (presumably depending on the ligand present) if only some of the porphyrin is found as $XMn^{III}(H_2O)TPP$, i.e., if both $XMn^{III}TPP$ and $XMn^{III}(H_2O)TPP$ are in favorable equilibrium. The addition of 2.5×10^{-3} M $XMn^{III}TPP$ did not increase the counts above that ($\sim$800 cpm, average) of the control (Table II). Thus, the porphyrins studied herein are not present as $XMn^{III}(H_2O)TPP$ in CCl_4. Variation of $[XMn^{III}TPP]$ from 0 to 2.5×10^{-3} M showed (Figure 1) no appreciable change in sample counts as the concentration of $XMn^{III}TPP$ was increased. It could be argued that addition of $XMn^{III}TPP$ to CCl_4 may decrease the solubility of H_2O in CCl_4 which would give similar results; we find it very unlikely, however, that 2.5×10^{-3} M $XMn^{III}TPP$ could decrease the solubility of H_2O in CCl_4 by a factor of 4 or 5 and that all of the $XMn^{III}TPP$ porphyrins act identically. These experiments do not preclude the possibility of $XMn^{III}(H_2O)TPP$ exisitng in other solvent systems (i.e., CH_3CN–H_2O) where the concentration of H_2O is orders of magnitude higher. For example, the equilibrium constants for the addition of H_2O to $ClMn^{III}TPP$ in aqueous acetone have been reported.[39] However, it should be noted that addition of small amounts of H_2O to dry CH_2Cl_2 solutions containing the more strongly ligated porphyrins ($XMn^{III}TPP$; $X^- = OCN^-$, F^-, Cl^-, Br^-, N_3^-) caused no observable change in the UV–vis spectrum. These experiments establish that under the experimental conditions employed for the oxygen transfer from p-CNDMANO to $XMn^{III}TPP$ in dry PhCN, the sixth position of $XMn^{III}TPP$ is free of (ligated) H_2O. This is important since traces of H_2O are present in solution, even in the rigorously dried PhCN solvent used herein for the kinetic experiments.

(39) Neya, S.; Morishima, I.; Yonezawa, T. *Biochemistry* **1981**, *20*, 2610–14.

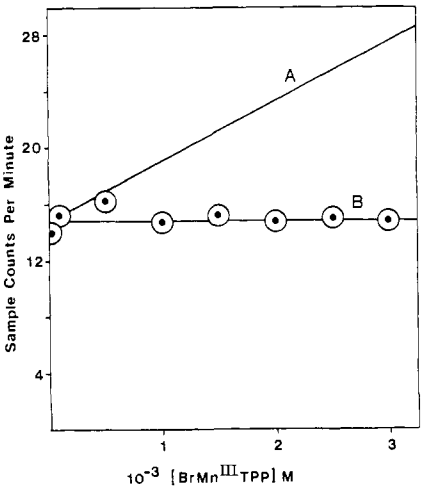

Figure 1. Dependence of sample counts per minute on the concentration of $BrMn^{III}TPP$. Curve A is expected if the porphyrin exists as $BrMn^{III}(H_2O)TPP$; curve B is expected if $BrMn^{III}TPP$ does not ligate a water molecule. The intercept of this plot is due to the solubility of H_2O (and TOH) in CCl_4 and is dependent on the TOH activity level used. The solubility limit of $BrMn^{III}TPP$ in CCl_4 at room temperature is approximately 3×10^{-3} M.

Table III. Product Yields for Reaction of $XMn^{III}TPP$ with *p*-CNDMANO and CH-ene in PhCN at 23.5 °C Expressed as a Percentage of $[p\text{-CNDMANO}]_0$

$XMn^{III}TPP$	CH-epox	*p*-CNMMA	CH-enol
F^-	38	52	
Cl^-	39	55	
Br^-	31	65	
I^-	20	28	6
OCN^- [a]	35	*e*	2
OCN^- [b]	35	39	3
OCN^- [c]	36	*e*	1
OCN^- [d]	33	*e*	

[a] $[p\text{-CNDMANO}]_0 = 4 \times 10^{-2}$ M. [b] $[p\text{-CNDMANO}]_0 = 2 \times 10^{-2}$ M. [c] $[p\text{-CNDMANO}]_0 = 1 \times 10^{-2}$ M. [d] $[p\text{-CNDMANO}]_0 = 5 \times 10^{-3}$ M. [e] Values not determined.

Ligand interchange (where ligands $X^- = Cl^-$, F^-, or N_3^-) between different Mn porphyrins ($XMn^{III}TPP$, $XMn^{III}MeOTPP$, and $XMn^{III}CAPTPP$) in dry PhCN (see Experimental Section for details) occurs at rates which are orders of magnitude greater than the rates of epoxidation or demethylation reported herein. That the Mn C_2-capped porphyrin also undergoes rapid ligand interchange indicates that the mechanism must be dissociative since backside addition of X^- to an $XMn^{III}CAPTPP$ is prevented by the blocking cap (see Introduction). In view of this rapid exchange, all kinetic measurements were carried out under reaction conditions where sources of extraneous or adventitious ligands were minimized.

Product Yields. Reaction of $XMn^{III}TPP$ with *p*-CNDMANO and excess cyclohexene (CH-ene) in PhCN (23.5 °C) gave three major oxidation products [cyclohexene epoxide (CH-epox), *p*-cyano-*N*-methylaniline (*p*-CNMMA), and *p*-cyano-*N*,*N*-dimethylaniline (*p*-CNDMA)] and cyclohexen-3-ol (CH-enol) as a minor product (eq 2). Although the 10% Carbowax 20–5% KOH column was suitable for the detection of *p*-cyanoaniline (p-CNA), none was found in any of the experiments reported herein, indicating that demethylation of *p*-CNMMA does not

occur. Inspection of Table III shows the product compositions and their dependence upon ligand, X^-, present in $XMn^{III}TPP$.

Inspection of Table III shows that the sum of the major oxidized species (CH-epox, *p*-CNMMA, and CH-enol) for most of the porphyrins is slightly less (~90%) than the amount of "oxene" available from $[p\text{-CNDMANO}]_0$. This is not due to quenching the reaction (with CS_2) prior to its completion. Loss of "oxene" could conceivably be due to oxidation of the solvent or traces of impurity in the solvent and in the case of $X^- = I^-$ replacement of I^- by IO_3^-. Loss of "oxene-equivalent" from p-CNDMANO has also been observed in kinetic and product studies involving $XFe^{III}TPP$ species as catalysts and CH_2Cl_2 as solvent.[40] The mechanism of this "oxene-equivalent" loss is a subject of further investigation.

When the ligand X^- of $XMn^{III}TPP$ equals F^-, Br^-, Cl^-, or OCN^-, the spectra of $XMn^{III}TPP$ remained unchanged during the course of the reaction, whereas the spectrum for $IMn^{III}TPP$ gave way to a spectrum identical with that for $IO_3Mn^{III}TPP$ during the initial catalytic turnover of p-CNDMANO. In addition, the yield of major oxidation products was significantly less with $IMn^{III}TPP$ than that expected from the known amount of oxene per turnover supplied to the system by *p*-CNDMANO. The oxygens of *p*-CNDMANO can be fully accounted for in reaction of $IMn^{III}TPP$ with p-CNDMANO and CH-ene (eq 3) if one assumes

$$IMn^{III}TPP + p\text{-CNDMANO} + \text{CH-ene} \rightarrow HOMn^{III}TPP,\ IO_3^-,\ p\text{-CNDMA},\ p\text{-CNMMA},\ \text{CH-epox},\ \text{CH-enol} \quad (3)$$

the iodide ligand is oxidized to iodate as suggested by the disappearance of the $IMn^{III}TPP$ spectrum and appearance of a spectrum identical with that of $HOMn^{III}TPP$ or $IO_3Mn^{III}TPP$ (eq 4). (The Soret band for $IO_3Mn^{III}TPP$ obtained from reaction of a large excess of IO_3^- and $XMn^{III}TPP$ in a biphasic system (CCl_4/H_2O) is fortuitously similar to that for $HOMn^{III}TPP$ obtained by shaking $XMn^{III}TPP$ ($X^- = F^-$, Cl^-, Br^-, I^-) with CCl_4/H_2O.) Assuming a 0.5% leakage of reactive oxygen per catalytic turnover to the solvent, the oxene partitions as follows: CH-epox, 20%; *p*-CNMMA, 28%; CH-enol, 6%; IO_3^-, 30% (3 × 10%); $HOMn^{III}TPP$, 10%; and solvent loss, 5% (total 99%).

Discussion

In the present study, we show that the Mn^{III} moiety of the ligated Mn^{III} porphyrin catalytic species (i.e., $XMn^{III}TPP$ and $XMn^{III}CAPTPP$; $X^- = F^-$, Cl^-, Br^-, I^-, N_3^-, OCN^-) employed for oxygen transfer from *p*-cyano-*N*,*N*-dimethylaniline *N*-oxide (*p*-CNDMANO) is devoid of H_2O as a second axial ligand so that the Mn^{III} is pentacoordinated prior to reaction with *p*-CNDMANO. It is also established that ligand (i.e., X^-) interchange between two differing XMn^{III} porphyrin species is much more rapid than oxygen transfer from *p*-CNDMANO to $XMn^{III}TPP$ and $XMn^{III}CAPTPP$. Table III presents the dependence of product yields upon X^- in the $XMn^{III}TPP$-catalyzed oxygen transfer from *p*-CNDMANO to cyclohexene. Inspection of Table III shows that (with the exception of $X^- = I^-$) the yield of cyclohexene epoxide is not greatly dependent upon the nature of X^-.

Higher valent oxidizing species which possess two axial ligands such as $O{=}Mn^{V}(X)TPP$ or $\cdot O\text{-}Mn^{IV}(X)TPP$ (as opposed to species such as $O{=}Mn^{IV}TPP^+$) are presumably the active oxygen transferring intermediates. If oxygen transfer occurred from $O{=}Mn^{V}TPP^+$ there would be no dependence of product yields upon X^- ligands since they would not be present in the critical transition state. The XMn^{III} C_2-cap-porphyrin can only form $O{=}Mn^{V}C_2$-cap-porphyrin after loss of Cl^- (which is very rapid; vide infra). That X^- must be attached to the Mn moiety during the course of the reaction is demonstrated by the lack of reactivity of XMn^{III} C_2-cap-porphyrin as catalyst. What is found is that this manganese porphyrin is very reluctant to catalyze O-transfer. Thus, reaction of 0.002 M $ClMn^{III}CAPTPP$ with 0.02 M *p*-CNDMANO and 2 M CH-ene in PhCN for several weeks resulted in the formation of barely detectable amounts of CH-epox (Figure 2).

(40) Nee, M.; Bruice, T. C., unpublished results.

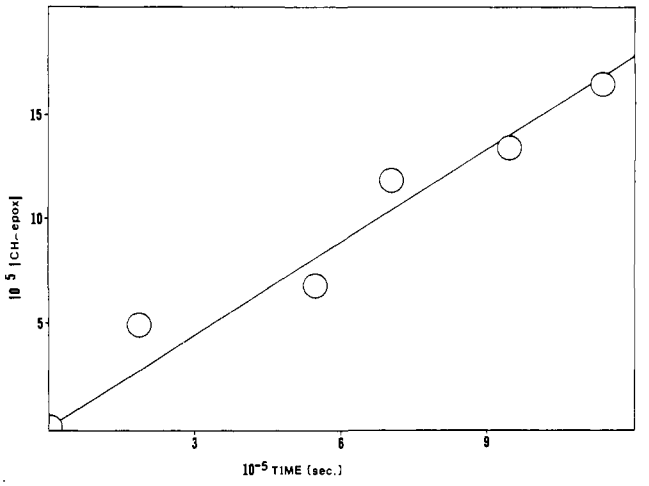

Figure 2. Initial time course for $ClMn^{III}CAPTPP$-catalyzed CH-epox formation from CH-ene and *p*-CNDMANO in PhCN at 23.5 °C. Total time required for ~1% of CH-epox formation was 2 weeks; reaction of $ClMn^{III}CAPTPP$ was slower by a factor of $>10^3$ than reaction of $ClMn^{III}TPP$ under identical reaction conditions.

The somewhat larger percentage yields of *p*-CNMMA as compared to CH-epoxy (Table III) may be accounted for by assuming the bimolecular rate constant for demethylation (k_{dm}) by the active oxygen species (i.e., $O{=}Mn^{V}(X)TPP$) is much greater than the rate of epoxidation (k_{epox}) by this species (eq 4).

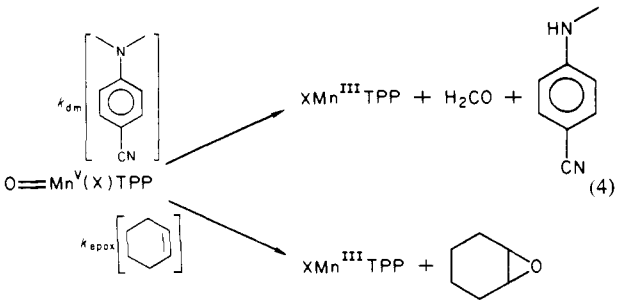

(4)

Alternatively, the greater yields of demethylated product may reflect: (i) the reaction of *p*-CNDMA with $O{=}Mn^{V}(X)TPP$ prior to its diffusion away from the {p-CNDMANO·$Mn^{III}(X)TPP$} complex formed after O-transfer from *p*-CNDMANO to $XMn^{III}TPP$ (eq 5) or (ii) the contribution of a concerted reaction

$$p\text{-CNDMANO} + XMn^{III}TPP \rightarrow\rightarrow \{NC\text{-}C_6H_4XNMe_2\cdot O{=}Mn^{V}(X)TPP\} \rightarrow p\text{-CNMMA} + CH_2O + XMn^{III}TPP \quad (5)$$

of *p*-CNDMANO with $XMn^{III}TPP$ in which $O{=}Mn^{V}(X)TPP$ is not formed. Since [CH-ene] is at least $10^3\times$ greater than [*p*-CNDMA], the relatively similar yields of *p*-CNDMMA and CH-epox indicate that either (i) $k_{dm} > 10^3 k_{epox}$ or (ii) the *p*-CNDMANO·$Mn^{III}(X)TPP$ complex partitions approximately equally to give *p*-CNMMA + CH_2O + $XMn^{III}TPP$ and *p*-CNDMA + free $O{=}Mn^{V}(X)TPP$, the latter of which is then trapped primarily by CH-ene to give $XMn^{III}TPP$ + CH-epox (eq 6).

Details of the mechanism were determined by following the time course of $XMn^{III}TPP$-catalyzed cyclohexene epoxide and *p*-cyano-*N*-methylaniline formation (23.5 °C, dry and anaerobic PhCN solvent) using quantitative gas chromatography. In most studies $[XMn^{III}TPP]_0 = 2 \times 10^{-3}$ M and $[p\text{-CNDMANO}]_0 = 2 \times 10^{-2}$ M so that 10 catalytic turnovers would be involved. In order to facilitate sample analysis, aliquots of reaction solution were quenched with CS_2 to convert unreacted *p*-CNDMANO to

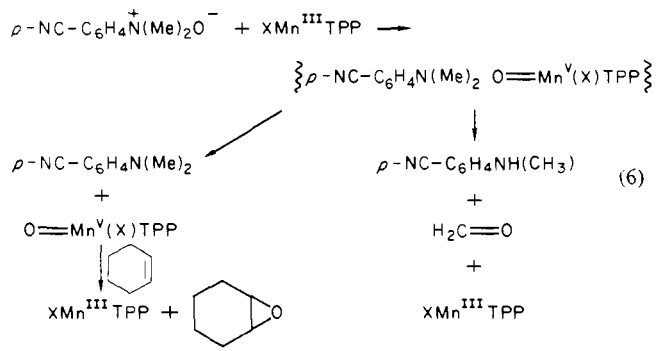

p-CNDMA. Thus [*p*-CNDMA] was observed to decrease during the course of the reaction such that [*p*-CNDMA] equals the initial concentration of *p*-CNDMANO used (0.02 M) at $t = 0$ (complete conversion of p-CNDMANO to *p*-CNDMA by CS_2 quench) and equals [*p*-CNDMA] formed from *p*-CNDMANO during the reaction at $t = \infty$ ($[p\text{-CNDMANO}]_\infty = 0$). The sum of $[p\text{-CNMMA}]_t + [p\text{-CNDMA}]_t \simeq 0.02$ M during the entire course of the reaction. We have analyzed the time courses for the formation of CH-epoxy and *p*-CNMMA from p-CNDMANO and CH-ene in the presence of $XMn^{III}TPP$ and are able to show for the chemically reasonable reaction sequences of Schemes I–III that only the last can fully account for: (i) the initial time course of CH-epox and p-CNMMA formation; (ii) the time dependence of the concentrations of CH-epoxy, *p*-CNMMA, and $XMn^{III}TPP$; (iii) the virtual inability of $ClMn^{III}CAPTPP$ to act as a catalyst for either demethylation or epoxidation; and (iv) dependence of the kinetics for epoxidations upon $[p\text{-CNDMANO}]_0$.

Dissociation of X^- from $XMn^{III}TPP$ in dry PhCN is significantly faster than the rates of demethylation or epoxidation as demonstrated by the rapid rates of ligand exchange observed in this study (see Experimental Section). That $XMn^{III}CAPTPP$ also undergoes rapid ligand interchange indicates that the exchange mechanism must be dissociative (eq 7) and not bimolecular (eq

$$XMn^{III}TPP \rightleftharpoons Mn^{III}TPP^+ + X^- \quad (7)$$

8). The capped porphyrin is unable to undergo backside-ligand

$$XMn^{III}TPP + X'Mn^{III}MeOTPP \underset{\text{(bimol)}}{\not\rightleftharpoons} X'Mn^{III}TPP + XMn^{III}MeOTPP \quad (8)$$

displacement due to the blocking cap structure. Reaction of $Mn^{III}TPP^+$ (formed by ligand dissociation) with *p*-CNDMANO to give CH-epox and *p*-CNMMA (Scheme I) would be expected to give rates which are dependent on the nature of X since the rates of dissociation of X^- from $XMn^{III}TPP$ are presumably dependent upon the nature of X^-. Additional evidence in favor of an X^--ligated active oxo species comes from comparing the relative rates of epoxidation of CH-ene by $ClMn^{III}TPP$ or $ClMn^{III}CAPTPP$ under the same experimental conditions. Ligand dissociation of $ClMn^{III}CAPTPP$ followed by oxygen transfer could give $O{=}Mn^{IV}CAPTPP$ where oxygen occupies the axial metal site which X^- vacated. If Scheme I were correct, the lack of backside solvent–metal interaction should make this species a relatively reactive oxene donor. This is not found to be so (loc. cit.). Similarly, a scheme involving a kinetically competent di-(*p*-CNDMANO)$Mn^{IV}TPP$ complex analogous to that isolated by Smegal and Hill[14] for the reaction of $ClMn^{III}TPP$ with iodosobenzene can also be discounted for the reactions of $XMn^{III}TPP$ with *p*-CNDMANO. That $XMn^{III}CAPTPP$ ($X^- = Cl^-, Br^-, N_3^-$) can form a complex with *p*-CNDMANO is shown by the decrease in the absorbance of the Soret band in a solution 5×10^{-5} M in Mn porphyrin when in the presence of 0.2 M *p*-CNDMANO. Complexation must occur by prior dissociation of X^-. Since, at concentrations employed for kinetic studies (1×10^{-3} M Mn porphyrin, 0.02 M *p*-CNDMANO) reaction of *p*-CNDMANO with $XMn^{III}CAPTPP$ is not observed, the equilibrium constant (K_e = [X^-][*N*-oxide complex]/[$XMn^{III}CAPTPP$][*p*-CNDMANO]) must be in the range of 10^{-4}. Thus, any competent kinetic scheme must account for all these observations and include an

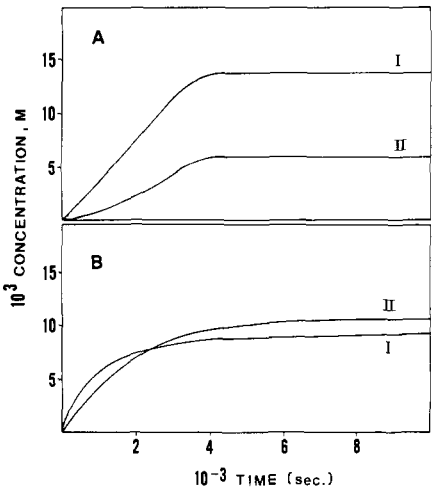

Figure 3. (A) Calculated time courses of CH-epox (I) and *p*-CNMMA (II) formation by the reaction sequences of Scheme II; the rate constants (M^{-1} s^{-1}) used to generate these curves are $k_1 = 20$, $k_{-1} = 5 \times 10^{-1}$, $k_2 = 1 \times 10^{-1}$, $k_3 = 1 \times 10^{-3}$. (b) Calculated time courses for CH-epox and p-CNMMA formation by the reaction sequences of Scheme II; the rate constants (M^{-1} s^{-1}) used to generate these curves are $k_1 = 5 \times 10^{-1}$, $k_{-1} = 100$, $k_2 = 100$, $k_3 = 2 \times 10^{-1}$.

Scheme I

$$XMn^{III}TPP \rightleftharpoons Mn^{III}TPP^+ + X^-$$

$$Mn^{III}TPP^+ + p\text{-CNDMANO} \longrightarrow \text{products by any sequence}$$

Scheme II

$$XMn^{III}TPP + p\text{-CNDMANO} \rightleftharpoons O{=}Mn^{V}(X)TPP + p\text{-CNDMA}$$

$$O{=}Mn^{V}(X)TPP + p\text{-CNDMA} \longrightarrow XMn^{III}TPP + p\text{-CNMMA} + CH_2O$$

$$O{=}Mn^{V}(X)TPP + \text{CH-ene} \longrightarrow XMn^{III}TPP + \text{CH-epox}$$

$$O{=}Mn^{V}(X)TPP \longrightarrow XMn^{III}TPP \text{ (loss of O to solvent)}$$

Scheme III

$$XMn^{III}TPP + p\text{-CNDMANO} \underset{k_{-1}}{\overset{k_1}{\rightleftharpoons}} p\text{-CNDMANO}\cdot Mn^{III}(X)TPP$$

$$p\text{-CNDMANO}\cdot Mn^{III}(X)TPP \underset{k_{-2}}{\overset{k_2}{\rightleftharpoons}} O{=}Mn^{V}(X)TPP + p\text{-CNDMA}$$

$$p\text{-CNDMANO}\cdot Mn^{III}(X)TPP \xrightarrow{k_3} XMn^{III}TPP + p\text{-CNMMA} + CH_2O$$

$$O{=}Mn^{V}(X)TPP + \text{CH-ene} \xrightarrow{k_4} XMn^{III}TPP + \text{CH-epox}$$

$$O{=}Mn^{V}(X)TPP \xrightarrow{k_5} XMn^{III}TPP \text{ (loss of O to solvent)}$$

active oxo species with the X^- ligand attached. Schemes II–III satisfy these criteria.

Reversible reaction of $XMn^{III}TPP$ and *p*-CNDMANO to give the reactive oxo species $O{=}Mn^{V}(X)TPP$ followed by reaction of this species with *p*-CNDMA and CH-ene cannot (as shown by digital simulation of Scheme II) reproduce the time courses for formation of CH-epoxy and p-CNMMA regardless of the value for the initial equilibrium constant. Computer simulation shows that if the equilibrium in Scheme II should favor product formation and the subsequent two steps are rate determining, then formation of CH-epoxy would be nearly zero-order and independent of $[p\text{-CNDMANO}]_0$ while the time course for the appearance of *p*-CNMMA would show a significant lag phase. This delay occurs because the initial concentration of *p*-CNDMA is low before its accumulation as a consequence of reaction of $O{=}Mn^{V}(X)TPP$ with CH-ene in multiple turnovers (Figure 3A). Alternatively, simulation of the reaction sequence of Scheme II with a more endothermic preequilibrium followed by somewhat faster rates of demethylation and epoxidation results in a plot for p-CNMMA

Table IV. Summary of Rate Constants for Kinetic Simulation of Experimental Data to Scheme III

	minimum allowed values[a]					minimum allowed values[b]	
$XMn^{III}TPP$	k_1 (M^{-1} s^{-1})	k_{-1} (s^{-1})	k_2 (s^{-1})	k_{-2} (M^{-1} s^{-1})	k_3 (s^{-1})	k_4 (M^{-1} s^{-1})	k_5 (s^{-1})
$ClMn^{III}TPP$	4×10^{-2}	1×10^{-2}	3.6×10^{-3}	0	3.7×10^{-3}	2.5×10^{-4}	1.5×10^{-4}
$BrMn^{III}TPP$	6.5×10^{-2}	1×10^{-2}	4.9×10^{-3}	0	9.5×10^{-3}	2.0×10^{-4}	5.0×10^{-5}
$OCNMn^{III}TPP$	7×10^{-1}	1×10^{-1}	7.1×10^{-2}	0	4.4×10^{-2}	5.6×10^{-3}	8.2×10^{-3}
$FMn^{III}TPP$	1.5	5×10^{-4}	5.6×10^{-5}	0	5.6×10^{-5}	4.0×10^{-4}	3.0×10^{-4}
$IMn^{III}TPP$[c]	8×10^{-1}	8×10^{-2}	3.2×10^{-2}	0	1.2×10^{-2}	1.5×10^{-3}	1.0×10^{-2}
$N_3Mn^{III}TPP$[c]	5.0	5×10^{-1}	6×10^{-2}	0	4.4×10^{-2}	1.3×10^{-2}	1×10^{-1}

[a] The values of k_{-1} are minimal given the values of k_2. The ratio of k_1/k_{-1} is critical, and for this reason the values of k_1 are also minimal. [b] The values of k_4 are minimal (step is not rate determining) and provide the best fits to the initial portion of the plots (Figure 4-6). The total fits of the curves are dependent upon k_4/k_5, and so the values of k_5 are also minimal. [c] The rate constants offered here should not be associated with the reactivity of $IMn^{III}TPP$ or $N_3Mn^{III}TPP$ since the ligands I^- and N_3^- are replaced during the initial turnovers of *p*-CNDMANO.

formation of the correct shape but the predicted plot of CH-epoxy formation vs. time (Figure 3B) was not satisfactory. In this case the initial rate for epoxidation is predicted to be greater than the initial rate for *p*-CNMMA formation, even though $[p\text{-CNMMA}]_\infty > [\text{CH-epoxy}]_\infty$. This, in turn, results in the prediction that the plots for appearance of p-CNMMA and CH-epox should cross. That this is not observed suggests that Scheme II is too simplistic. Further evidence against such a simple scheme can be inferred from the complete lack of *p*-CNA formation. If $O{=}Mn^{V}(X)TPP$ reacted bimolecularly with *p*-CNDMA to give *p*-CNMMA and $XMn^{III}TPP$, then one might expect that p-CNMMA formed during the course of reaction would compete to some extent for the reactive Mn^{V}-oxo species since [*p*-CNDMA] ≃ [*p*-CNMMA] within a factor of 2 at 50–75% reaction for most $XMn^{III}TPP$ species.

Incorporation of a reactive intermediate (drawn for convenience as p-CNDMANO·$Mn^{III}(X)TPP$) into the reaction sequences (Scheme III) permits a quantitative analysis of the multiple turnover reaction, providing a step is included to account for loss of "oxene" to the solvent. This extra reaction is only a minor approximation for some of the porphyrins studied ($XMn^{III}TPP$; $X^- = F^-$, Cl^-, Br^-, and to a lesser extent OCN^-) since $[p\text{-CNMMA}]_\infty + [\text{CH-epoxy}]_\infty$ nearly equaled $[p\text{-CNDMANO}]_0$ for reactions with these catalysts. This is not the case for $IMn^{III}TPP$. In the case of $IMn^{III}TPP$, approximately 30% of the "oxene" is used to convert I^- to IO_3^-.

Loose complex formation between $XMn^{III}TPP$ ($X^- = Cl^-$, Br^-, OCN^-) and p-CNDMANO is quite plausible since the radiometric measurements reported herein demonstrate that H_2O does not bind strongly to the sixth axial ligand position of $XMn^{III}TPP$ in aprotic solvents—and presumably neither does p-CNDMANO. This lack of strong binding in the reaction of $XMn^{III}TPP$ and p-CNDMANO in PhCN is also supported by the observation that only a partial disappearance of the $XMn^{III}TPP$ Soret band occurs upon mixing *p*-CNDMANO (final concentration 0.2 M) and $XMn^{III}TPP$ (final concentration 5×10^{-5} M). The $XMn^{III}TPP$ Soret band decreased ~10–50%, where the amount of decrease depends on the porphyrin ligand. For example, $OCNMn^{III}TPP$ showed only a small change (~10%) in o.d. at λ 474 nm on addition of *p*-CNDMANO, whereas the $BrMn^{III}TPP$ Soret band at λ 484 nm decreased fairly rapidly to approximately 50% of its original peak height. The decrease in $XMn^{III}TPP$ Soret band absorbance is accompanied by an increase in a band at λ 444 nm. That $XMn^{III}CAPTPP$ ($X^- = Cl^-$, I^-, N_3^-) undergoes somewhat similar spectral changes in PhCN suggests that the decrease in the $XMn^{III}TPP$ Soret band is not only due to formation of the *p*-CNDMANO·$Mn^{III}(X)TPP$ complex or $O{=}Mn^{V}(X)TPP$, but to replacement of the X^- ligand by p-CNDMANO. The ligand interchange experiments reported herein (Experimental Section) favor a ligand predissociation mechanism (eq 9 and 10).

$$XMn^{III}CAPTPP \rightleftharpoons X^- + Mn^{III}CAPTPP^+ \quad (9)$$

$$Mn^{III}CAPTPP + p\text{-CNDMANO} \rightleftharpoons (p\text{-CNDMANO})Mn^{III}CAPTPP \quad (10)$$

Although these nonproductive equilibria are seen when $[XMn^{III}TPP] = 5 \times 10^{-5}$ M and [*p*-CNDMANO] = 0.2 M, they are not expected to affect the reaction sequences of Scheme III since ~10^2-fold higher $XMn^{III}TPP$ concentrations and 10-fold concentrations of p-CNDMANO were employed in the kinetic studies. Scheme III, which neglects such nonproductive pathways, predicts that [$XMn^{III}TPP$] should quickly decrease by approximately 10–20% (depending on the porphyrin) after which it should slowly return during the course of the reaction. This is what has been observed spectrally.

The lack of reactivity of the chloro-capped porphyrin may be due to one or both of the following features. In order for *p*-CNDMANO to complex with $ClMn^{III}CAPTPP$, the Cl^- ligand must be displaced. This process is thermodynamically less favorable (eq 11) than is complexation of *p*-CNDMANO with

$$ClMn^{III}CAPTPP + p\text{-CNDMANO} \xrightleftharpoons{K \sim 10^{-4}} Cl^- + (p\text{-CNDMANO})Mn^{III}CAPTPP \quad (11)$$

$$ClMn^{III}TPP + p\text{-CNDMANO} \xrightleftharpoons{K \sim 1\text{–}10\ M^{-1}} (p\text{-CNDMANO})Mn^{III}(Cl)TPP \quad (12)$$

$ClMn^{III}TPP$ (eq 12). Thus the lack of reactivity of capped porphyrin as an oxygen transfer agent may be due, at least in part, to the very low concentration of (*p*-CNDMANO)·$Mn^{III}CAPTPP$ complex. Secondly, the reactivity of this latter complex may be intrinsically very slow in the absence of the sixth axial ligand, X^-. Investigations are in progress to verify these points.

Partitioning of the *p*-CNDMANO·$Mn^{III}(X)TPP$ intermediate in Scheme III occurs to regenerate the reactants or to afford either *p*-CNMMA + $XMn^{III}TPP$ + CH_2O or a reactive oxo species ($O{=}Mn^{V}(X)TPP$) + *p*-CNDMA (as shown in eq 6). The Mn^{V} species subsequently reacts with the CH-ene to regenerate the catalyst, $XMn^{III}TPP$, and CH-epox. Such a scheme predicts that the ratio of initial rates for *p*-CNMMA and CH-epox formation should be identical with the product ratio providing $O{=}Mn^{V}(X)TPP$ is rapidly scavenged by CH-ene. Good agreements between the reaction scheme simulation and time dependence of CH-epoxy and *p*-CNDMA formation were obtained using $ClMn^{III}TPP$, $BrMn^{III}TPP$ and $OCNMn^{III}TPP$ as catalysts (Figure 4A–C). In Figure 5 there is displayed fits of Scheme III to plots of the time dependence of formation of CH-epox as a function of $[p\text{-CNDMANO}]_0$ using $OCNMn^{III}TPP$ as catalyst. The plots for product formation with time, when using $FMn^{III}TPP$ as catalyst, are unusual. The fit of Scheme III in this case is shown in Figure 4D. Examination of Figure 4D shows that product appearance is apparently zero order in contrast to the more first-order appearing product formation for other $XMn^{III}TPP$ species.

The rate constants used in the simulations are listed in Table IV. The slight induction period (Figure 4C) for $BrMn^{III}TPP$-catalyzed CH-epox formation was simulated by use of a k_4 value which made epoxide formation more rate determining in the initial stages of the reaction. We found that a better simulation of the experimental data was obtained when using values of $k_{-2}[p\text{-CNDMA}]$ less than k_4[CH-ene], i.e., primarily loss of $O{=}Mn^{V}TPPX$ by rapid reaction with alkene. Under our experimental conditions where *p*-CNDMA was not added to the reaction solution, a value of $k_{-2} = 0$ gave satisfactory simulated curves for

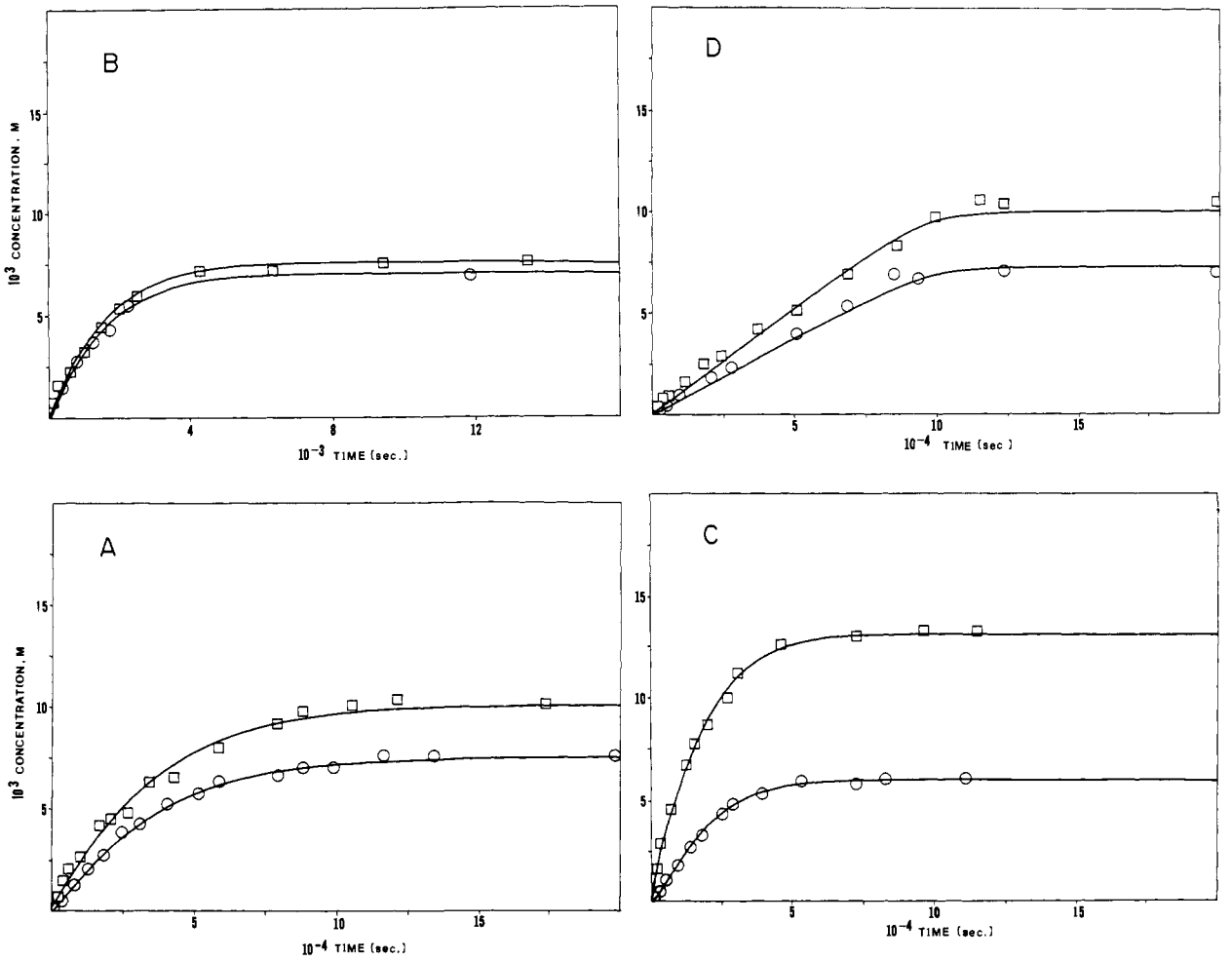

Figure 4. The fitting of experimental points for the formation of CH-epox (○) and *p*-CNMMA (□) from *p*-CNDMANO and CH-ene in PhCN at 23.5 °C by computer similation of Scheme III: (A) $ClMn^{III}TPP$ catalysis, (B) $OCNMn^{III}TPP$ catalysis, (C) $BrMn^{III}TPP$ catalysis, (D) $FMn^{III}TPP$ catalysis.

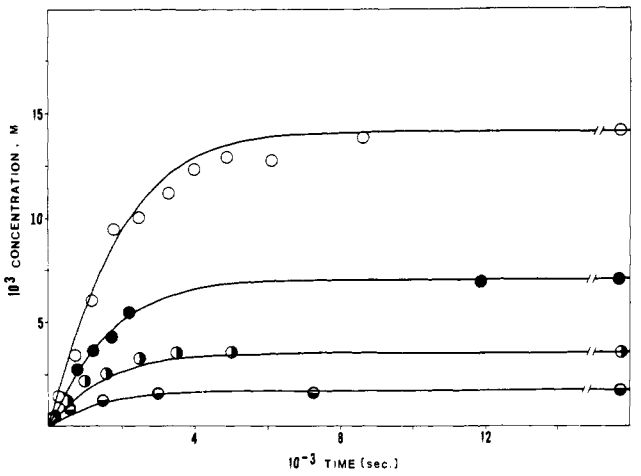

Figure 5. Dependence of the initial *p*-CNDMANO concentration on the simulated (Scheme III) and experimentally observed time courses for $OCNMn^{III}TPP$-catalyzed epoxidation of CH-ene. The concentrations (M) of *p*-CNDMANO used were: (○) 4×10^{-2}, (●) 2×10^{-2}, (◑) 1×10^{-2}, (◒) 5×10^{-3}. The simulated time courses were generated using the rate constants given in Table IV.

CH-epoxy and *p*-CNMMA formation and so we have used $k_{-2} = 0$ for simplicity. If addition of p-CNDMA to the reaction solution resulted in inhibition of epoxidation, then k_{-2} would have a small but finite value. It is important to note that the absolute values of k_1, k_{-1}, k_4, and k_5 do not strongly affect the calculated reaction course providing k_1/k_{-1} and k_4/k_5 have stringent values. For example, reaction scheme simulation of $ClMn^{III}TPP$ with *p*-CNDMANO and CH-ene using $k_1 = 4\ M^{-1}\ s^{-1}$ and $k_{-1} = 1\ s^{-1}$ (100× larger than the values offered in Table IV for this reaction) gives an identical time course for CH-epox and *p*-CNMMA formation when slightly smaller values of k_2 and k_3 are used ($k_2 = 2.28 \times 10^{-3}\ s^{-1}$, $k_3 = 2.6 \times 10^{-3}\ s^{-1}$). The fits of the curves are altered by changes of only a few percent in the value of k_1/k_{-1}, k_4/k_5, k_2, and k_3. Unfortunately, the influence of X^- upon the rate (k_4) of epoxidation by $O{=}Mn^{V}(X)TPP$ cannot be determined independently. The values of k_4 in Table IV are minimal (the reaction is not rate determining).

Simulation of the $FMn^{III}TPP$ data shows that F^- as a ligand stabilizes (compared to $X^- = Cl^-, Br^-, OCN^-$) the p-CNDMA-NO·$Mn^{III}(X)TPP$ complex with respect to both reactants and the Mn^{V}–oxo species so that the concentration of this complex accumulated during catalytic turnover is greater than when X^- is an alternative ligand. The equilibrium constant for formation of *p*-CNDMANO·$Mn^{III}(F)TPP$ ($K = 3000\ M^{-1}$) is approximately 700× larger than that for *p*-CNDMANO·$Mn^{III}(Cl)TPP$ complex formation ($K = 4\ M^{-1}$) whereas the rate of demethylation when $X^- = F^-$ is approximately 70× smaller than for $X^- = Cl^-$. This increases the concentration of the fluoride complex over the chloride complex by an approximate factor of 10; this is enough to change the kinetics of CH-epox and *p*-CNMMA formation from apparent first order to zero order. The simulation for CH-epox formation shows less deviation than does the calculated *p*-CNMMA curve; this may be due to the lower reliability of the *p*-CNMMA analysis as indicated by the slight excess of methylated aniline formed over initial *N*-oxide concentration due to the GC calibration. It should be noted that $FMn^{III}TPP$ exhibits significantly different properties (i.e., spectra, solubilities, and time

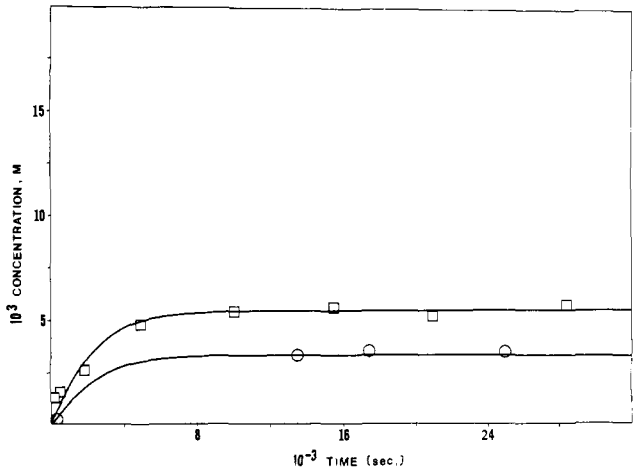

Figure 6. Simulated and observed time courses for $IMn^{III}TPP$-catalyzed formation of CH-epoxy (O) and *p*-CNMMA (□) from *p*-CNDMANO and CH-ene in PhCN at 23.5 °C.

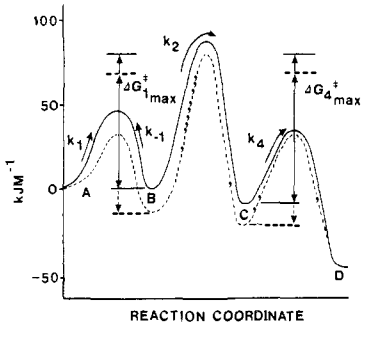

Figure 7. Reaction coordinate cartoons for the epoxidation of cyclohexene by *p*-CNDMANO catalyzed by $ClMn^{III}TPP$ (—) and $FMn^{III}TPP$ (---). Standard states of reactants at 1 M were used. States A, B, C, and D represent $XMn^{III}TPP$ + *p*-CNDMANO, *p*-CNDMANO-$Mn^{III}(X)TPP$, *p*-CNDMA + $O{=}Mn^{V}(X)TPP$ + cyclohexene, and $XMn^{III}TPP$ + cyclohexene epoxide, respectively. The values of $\Delta G^{\ddagger}_{1max}$ and $\Delta G^{\ddagger}_{4max}$ have been calculated from the minimum values of k_1, k_{-1}, and k_4 (Table IV) used for computer simulation. The barrier heights for $\Delta G^{\ddagger}_1$ and $\Delta G^{\ddagger}_4$ have been sketched. These steps are not rate limiting but must possess values which do not exceed $\Delta G^{\ddagger}_{1max}$ and $\Delta G^{\ddagger}_{4max}$. The heights of the ground states (relative to A) have been calculated from k_1/k_{-1} for B, k_4 and the maximum barrier height (i.e., $\Delta G^{\ddagger}_{max}$) for C. The energy content of *D* has been set below that of A as befits an exergonic reaction. The reaction B → C (i.e., formation of $O{=}Mn^{V}(X)TPP$) is rate determining.

course for epoxidation and demethylation) than the other porphyrins studied.

Reaction of $IMn^{III}TPP$ with *p*-CNDMANO in the presence of CH-ene can also be fitted using the reaction sequences of Scheme III (Figure 6). However, the I^- ligand is displaced from the porphyrin during the initial course of the reaction and the final Mn^{III} porphyrin spectrum is distinctly different from the spectrum of $IMn^{III}TPP$. The final spectrum obtained at completion of the kinetic run with $IMn^{III}TPP$ is strikingly similar to the spectrum of $IO_3Mn^{III}TPP$ or $HOMn^{III}TPP$. This observation plus the oxygen balance (Results) suggests that the I^- ligand is oxidized to a IO_3^- ligand early in the catalytic turnover of p-CNDMANO. Further evidence for I^- ligand replacement or oxidation in the early part of the reaction comes from a comparison of the initial rates of $IMn^{III}TPP$-catalyzed epoxidiation or demethylation with the other halo-Mn^{III} porphyrins. With $IMn^{III}TPP$ turnover of *p*-CNDMANO is approximately 20× faster than with other $XMn^{III}TPP$ (X^{-1} = F^-, Cl^-, Br^-) species. The ease of I^- oxidation as compared with the other halides corroborates this observation.

Conclusion

The $XMn^{III}TPP$ complexes accept the oxygen of *p*-cyano-*N*,*N*-dimethylaniline *N*-oxide as "oxene" to generate $O{=}Mn^{V}(X)TPP$. The rate constants for this "oxene" transfer have been shown to be dependent upon the ligand X^-. The rate constants for "oxene" transfers from $O{=}Mn^{V}(X)TPP$ species to cyclohexene are not rate determining so that only minimal value for these rate constants can be assigned and, thus, the influence of the ligand X^- on these rates cannot be discerned. Demethylation of *p*-cyano-*N*,*N*-dimethylaniline *N*-oxide occurs within a complex of this species with $XMn^{III}TPP$ (eq 6) and not in a bimolecular reaction of the separate entities *p*-cyano-*N*,*N*-dimethylaniline and $O{=}Mn^{V}(X)TPP$ formed after "oxene" transfer and diffusion apart (eq 4). In Figure 7 there is presented reaction coordinate cartoons for the epoxidation of cyclohexene when using $ClMn^{III}TPP$ and $FMn^{III}TPP$ as catalysts. The free energy of formation of the *p*-CNDMANO·$Mn^{III}(X)TPP$ complexes are calculable from the determined equilibrium constant k_1/k_{-1}, and from this and k_2 (Table IV) there is determined the free energy of the critical transition state which involves the formation of the $O{=}Mn^{V}(X)TPP$ species.

Acknowledgment. Funding for this research was from the National Institutes of Health and the American Cancer Society. M.F.P. expresses appreciation to the Natural Sciences and Engineering Research Council of Canada for a postdoctoral fellowship, and E.F.P. expresses gratitude to the Max Planck Society of West Germany for an Otto Hahn fellowship.

Registry No. *p*-CNDMANO, 62820-00-2; *p*-CNMMA, 4714-62-9; *p*-CNDMA, 1197-19-9; $ClMn^{III}TPP$, 32195-55-4; $BrMn^{III}TPP$, 55290-32-9; $OCNMn^{III}TPP$, 86549-48-6; $FMn^{III}TPP$, 89789-33-3; $IMn^{III}TPP$, 55290-33-0; $N_3Mn^{III}TPP$, 56413-47-9; $ClMn^{III}CAPTPP$, 89789-34-4; CH-ene, 110-83-8; CH-epox, 286-20-4; CH-enol, 822-67-3; cytochrome P-450, 9035-51-2; monooxygenase, 9038-14-6.